# Correction

**NEUROSCIENCE**

Correction for "Heterogeneity within the frontoparietal control network and its relationship to the default and dorsal attention networks," by Matthew L. Dixon, Alejandro De La Vega, Caitlin Mills, Jessica Andrews-Hanna, R. Nathan Spreng, Michael W. Cole, and Kalina Christoff, which was first published January 30, 2018; 10.1073/pnas.1715766115 (*Proc Natl Acad Sci USA* 115:E1598–E1607).

The authors note that Fig. 2 appeared incorrectly. The corrected figure and its legend appear below.

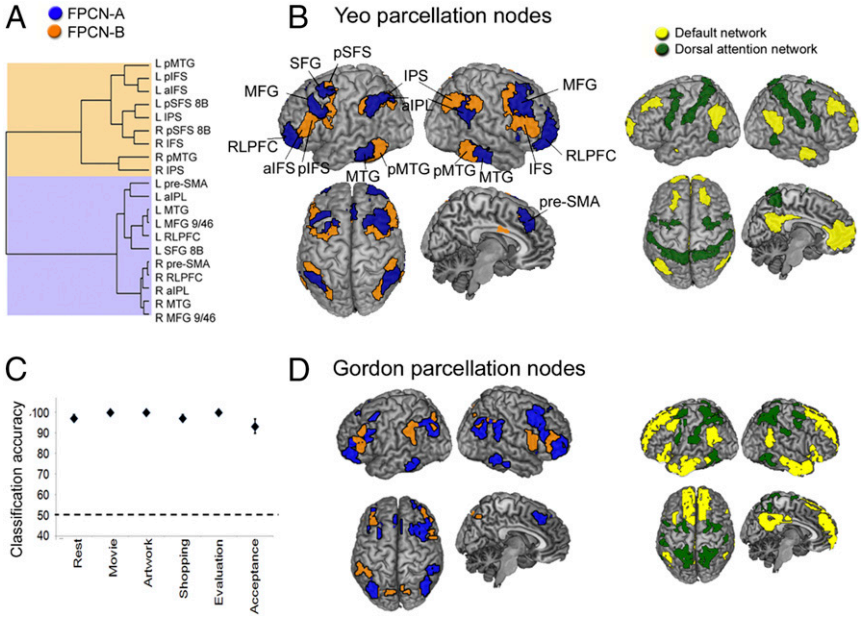


**Fig. 2.** FPCN fractionation based on internetwork connectivity with the DN and DAN. (*A*) Hierarchical clustering results based on intermodular connections. FPCN nodes cluster into two separate families. (*B*) Surface rendering of FPCN nodes from the Yeo parcellation, color-coded based on the hierarchical clustering results. (*C*) Accuracy of the support vector machine classifier in distinguishing $FPCN_A$ and $FPCN_B$ FC patterns with the DN and DAN during each condition. Dotted line represents baseline accuracy (50%). (*D*) Surface rendering of FPCN nodes from the Gordon parcellation, color coded based on the hierarchical clustering results in *SI Appendix*, Fig. S3*B*. Abbreviations are the same as in Fig. 1.



Published online March 12, 2018.

www.pnas.org/cgi/doi/10.1073/pnas.1803276115

# Heterogeneity within the frontoparietal control network and its relationship to the default and dorsal attention networks

Matthew L. Dixon[a,1], Alejandro De La Vega[b], Caitlin Mills[a], Jessica Andrews-Hanna[c], R. Nathan Spreng[d,e], Michael W. Cole[f], and Kalina Christoff[a,g,1]

[a]Department of Psychology, University of British Columbia, Vancouver, BC V6T 1Z4, Canada; [b]Department of Psychology, University of Texas at Austin, Austin, TX 78712; [c]Institute of Cognitive Science, University of Colorado at Boulder, Boulder, CO 80309-0345; [d]Laboratory of Brain and Cognition, Montreal Neurological Institute, Department of Neurology and Neurosurgery, McGill University, Montreal, QC H3A 2B4, Canada; [e]Human Neuroscience Institute, Department of Human Development, Cornell University, Ithaca, NY 14853-7601; [f]Center for Molecular and Behavioral Neuroscience, Rutgers University, Newark, NJ 08854; and [g]Centre for Brain Health, University of British Columbia, Vancouver, BC V6T 1Z4, Canada

Edited by Earl K. Miller, Massachusetts Institute of Technology, Cambridge, MA, and accepted by Editorial Board Member Michael S. Gazzaniga January 8, 2018 (received for review September 6, 2017)

**The frontoparietal control network (FPCN) plays a central role in executive control. It has been predominantly viewed as a unitary domain general system. Here, we examined patterns of FPCN functional connectivity (FC) across multiple conditions of varying cognitive demands, to test for FPCN heterogeneity. We identified two distinct subsystems within the FPCN based on hierarchical clustering and machine learning classification analyses of within-FPCN FC patterns. These two FPCN subsystems exhibited distinct patterns of FC with the default network (DN) and the dorsal attention network (DAN). $FPCN_A$ exhibited stronger connectivity with the DN than the DAN, whereas $FPCN_B$ exhibited the opposite pattern. This twofold FPCN differentiation was observed across four independent datasets, across nine different conditions (rest and eight tasks), at the level of individual-participant data, as well as in meta-analytic coactivation patterns. Notably, the extent of FPCN differentiation varied across conditions, suggesting flexible adaptation to task demands. Finally, we used meta-analytic tools to identify several functional domains associated with the DN and DAN that differentially predict activation in the FPCN subsystems. These findings reveal a flexible and heterogeneous FPCN organization that may in part emerge from separable DN and DAN processing streams. We propose that $FPCN_A$ may be preferentially involved in the regulation of introspective processes, whereas $FPCN_B$ may be preferentially involved in the regulation of visuospatial perceptual attention.**

frontoparietal control network | default network | dorsal attention network | cognitive control | functional connectivity

Modern neuroscientific investigations have demonstrated that frontoparietal cortices contribute to executive control and adaptive behavior via the flexible encoding of task demands and desired outcomes and the top-down modulation of processing in other brain regions (1–8). Despite this progress, we lack a clear understanding of the functional organization of frontoparietal cortex, a critical step in discerning the network architecture underlying executive control. Distributed frontoparietal regions often activate together in response to diverse task demands, suggesting that they may function as a unified, domain general control system, referred to as the frontoparietal control network (FPCN) or "multiple demand" system (4). It is possible, however, that a finer level of internal organization may be present within the FPCN, with distinct subsystems contributing to different types of executive control. Progress has been made in understanding other networks (e.g., default network) via fractionating them into distinct subsystems with unique functional roles (9). Existing models have distinguished the FPCN from networks centered on insular and cingulate cortices (e.g., "salience" and cingulo-opercular networks) (10, 11). However, possible functional heterogeneity within the FPCN has not been explored in detail.

In a seminal paper, Yeo et al. (12) introduced a 7-network parcellation that has had a considerable influence on the field of network neuroscience. In this 7-network parcellation, the FPCN appears as a uniform network. However, Yeo et al. also reported a fine-grained 17-network parcellation that has received much less attention in the literature. In this 17-network solution, the FPCN appears to be segregated into two distinct subsystems (see Yeo et al., figure 9). [The Yeo et al. 17-network parcellation actually divides the unified FPCN into three separate subnetworks; however, one subnetwork is only composed of two regions (the posterior cingulate and precuneus) and does not include a frontal component. As such, it is not a frontoparietal system per se, and is not examined here.] Moreover, recent work suggests that a FPCN fractionation can be observed in the data of individual participants (13). These findings represent important empirical evidence for heterogeneity within this network. However, prior work has not systematically investigated the basis of this FPCN fractionation or its functional implications.

## Significance

**The frontoparietal control network (FPCN) contributes to executive control, the ability to deliberately guide action based on goals. While the FPCN is often viewed as a unitary domain general system, it is possible that the FPCN contains a fine-grained internal organization, with separate zones involved in different types of executive control. Here, we use graph theory and meta-analytic functional profiling to demonstrate that the FPCN is composed of two separate subsystems: $FPCN_A$ is connected to the default network and is involved in the regulation of introspective processes, whereas $FPCN_B$ is connected to the dorsal attention network and is involved in the regulation of perceptual attention. These findings offer a distinct perspective on the systems-level circuitry underlying cognitive control.**

Author contributions: M.L.D. and K.C. designed research; M.L.D. performed research; J.A.-H., R.N.S., and M.W.C. contributed new reagents/analytic tools; M.L.D., A.D.L.V., and C.M. analyzed data; J.A.-H., R.N.S., M.W.C., and K.C. provided guidance on analyses; and M.L.D. wrote the paper.

The authors declare no conflict of interest.

This article is a PNAS Direct Submission. E.K.M. is a guest editor invited by the Editorial Board.



[1]To whom correspondence may be addressed. Email: mattdixon99@gmail.com or kchristoff@psych.ubc.ca.

This article contains supporting information online at www.pnas.org/lookup/suppl/doi:10.1073/pnas.1715766115/-/DCSupplemental.

Here, we used a hypothesis-driven approach together with graph theoretical analyses to examine the possibility that the fine-grained internal organization of the FPCN may be driven by specific connectional patterns as part of a "distance from sensorimotor processing" principle that defines global brain organization (14–17). The FPCN is extensively interconnected with both the default network (DN) and dorsal attention network (DAN) (18)—large-scale systems that contribute to distinct and sometimes competing modes of processing (19–23). The DAN has a close relationship with sensorimotor regions (12) and plays a key role in visuospatial perceptual attention (24–26). It contains neurons with spatially organized receptive fields (25, 27) that are activated during saccades (28), shifts of attention to salient objects in the external environment (29–31), and during visually guided reaching actions (24, 32). In contrast, the DN contributes to introspective processes that are, in some cases, independent from sensory input (14, 21, 33–35). Specifically, the DN is involved in mentalizing (36), autobiographical memory (37), spontaneous cognition (38–41), self-referential processing (42), and high-level aspects of emotion (34, 43, 44). Correspondingly, it has been demonstrated that the DN is further removed spatially and functionally from sensorimotor processing than the DAN (14). We hypothesized that the distinct DN and DAN processing streams may be carried forward into the organization and functions of the FPCN.

We first examined the network architecture of the FPCN using hierarchal clustering to determine whether FPCN nodes separate into distinct subsystems based on intramodular (within-network) connections. We then determined whether the observed subsystems exhibit topographically organized functional connections with the DN and DAN. That is, we predicted that FPCN regions coupled with the DN would be spatially distinct from FPCN regions coupled with the DAN. We investigated functional coupling patterns during rest and several different tasks, which allowed us to look for differences in coupling patterns that persist across different cognitive states. Second, to determine the generalizability of a putative FPCN fractionation related to the DN and DAN, we examined functional connectivity (FC) patterns in three additional independent datasets, and we examined meta-analytic coactivation patterns across 11,406 neuroimaging studies within the Neurosynth database (45). Third, we performed an individual-level network mapping analysis to examine the extent of interindividual variability in the spatial organization of FPCN subsystems. Fourth, we examined how the putative FPCN fractionation relates to task-related flexibility in FC patterns. Prior work has shown that network organization changes across time and context (46–50), with FPCN regions exhibiting considerable flexibility (7, 51, 52), consistent with a role in the context-dependent regulation of thought and perception (4, 6). Here, we investigated the relationship between FPCN heterogeneity and task-related flexibility. Finally, in an exploratory analysis, we used Neurosynth topic mapping to identify functional domains that differentially predict activation in the FPCN subsystems.

Our primary dataset involved data collected from 24 participants that underwent fMRI scanning during six separate conditions designed to elicit mental states similar to those frequently experienced in everyday life. These six conditions varied in the amount of introspective thought and perceptual demands, and included: (*i*) rest; (*ii*) movie viewing; (*iii*) analysis of artwork; (*iv*) social preference shopping task; (*v*) evaluation-based introspection; and (*vi*) acceptance-based introspection (see *Materials and Methods* for details). Additionally, we examined FC patterns in three other datasets involving traditional cognitive control tasks that are known to activate the FPCN: (*i*) rule use; (*ii*) Stroop; and (*iii*) 2-back working memory. Data were processed using standard techniques (53), and we did not use global signal regression, so as to avoid distorting FC values (54).

## Results

**Evidence for Distinct FPCN Subsystems.** Graph theory represents complex systems such as the brain as a graph consisting of a set of nodes (regions) and edges (connections between nodes), and allows for a quantitative description of network properties (55, 56). We calculated the time-series correlation between nodes spanning the DAN, DN, and FPCN based on the Yeo parcellation (12). We first analyzed the organization of FPCN nodes based solely on intramodular (within-network) FC patterns. We used hierarchical clustering to organize nodes into a tree structure based on the similarity of their FC profiles. The analysis revealed two clusters or subsystems that we refer to as $FPCN_A$ and $FPCN_B$ (Fig. 1 *A* and *B* and *SI Appendix*, Fig. S1). $FPCN_A$ and $FPCN_B$ nodes were, to some extent, spatially interleaved, similar to observations in prior work (12, 13). To examine whether the distinction between $FPCN_A$ and $FPCN_B$ FC patterns were consistent across participants, we used a linear support vector machine (SVM) classifier to distinguish $FPCN_A$ and $FPCN_B$ intramodular FC patterns in new participants based on data from other participants. The SVM attempts to find a hyperplane that best separates the two classes of data. We used k-fold cross-validation ($k = 4$), where the classifier was trained on data from 75% of participants, then tested on unlabeled data from the remaining 25% of participants. Using this procedure, we found highly accurate (>90%) discrimination of the $FPCN_A$ and $FPCN_B$ during every condition in the primary dataset (Fig. 1*C* and *SI Appendix*, Fig. S2). Permutation testing in which FPCN subsystem labels were randomly shuffled revealed

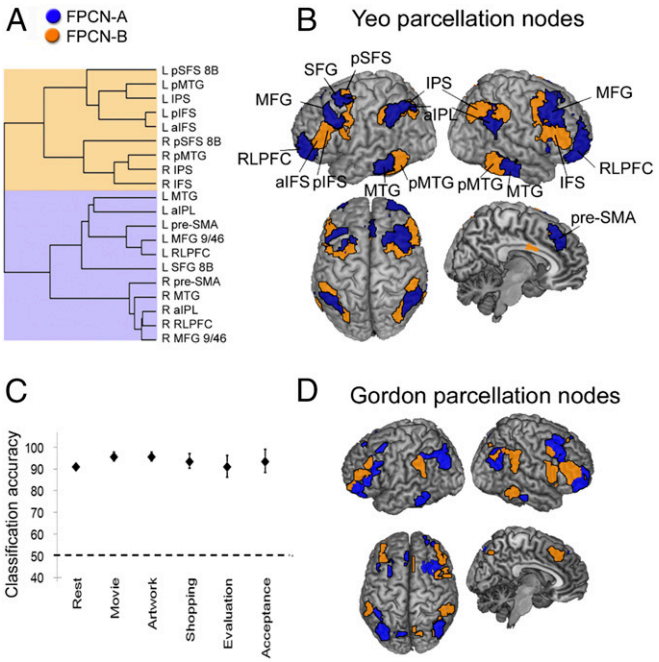


**Fig. 1.** FPCN fractionation based on intramodular connectivity. (*A*) Hierarchical clustering results based on intramodular (within-FPCN) connections. FPCN nodes cluster into two separate families. (*B*) Surface rendering of FPCN nodes from the Yeo parcellation, color-coded based on the hierarchical clustering results. (*C*) Accuracy of the support vector machine classifier in distinguishing $FPCN_A$ and $FPCN_B$ within-network FC patterns during each condition. Dotted line represents baseline accuracy (50%). (*D*) Surface rendering of FPCN nodes from the Gordon parcellation, color-coded based on the hierarchical clustering results in *SI Appendix*, Fig. S1*B*. Abbreviations: aIFS, anterior inferior frontal sulcus; aIPL, anterior inferior parietal lobule; IPS, intraparietal sulcus; MFG, middle frontal gyrus; MTG, middle temporal gyrus; pIFS, posterior inferior frontal sulcus; pMTG, posterior middle temporal gyrus; pre-SMA, presupplementary motor area; pSFS, posterior superior frontal gyrus; RLPFC, rostrolateral prefrontal cortex.

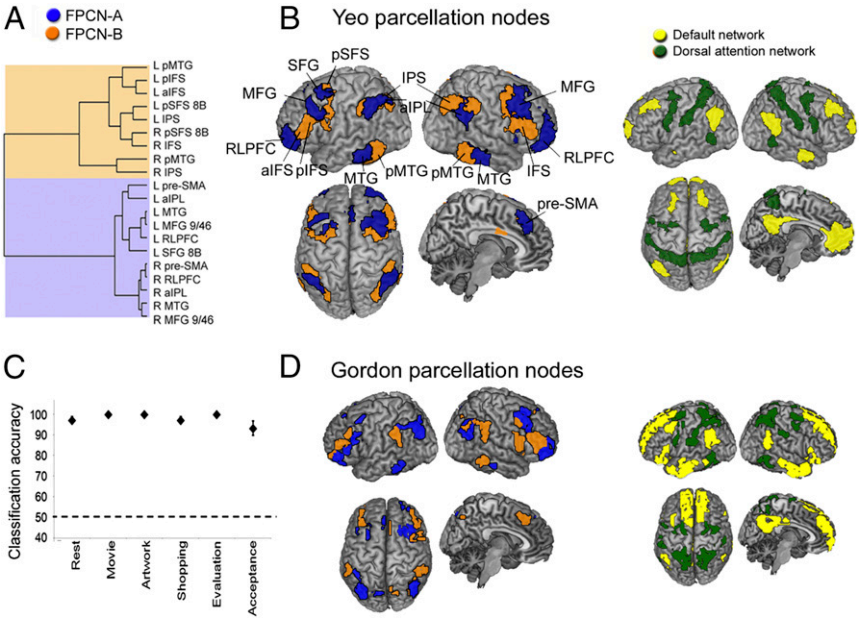


**Fig. 2.** FPCN fractionation based on inter-network connectivity with the DN and DAN. (*A*) Hierarchical clustering results based on intermodular connections. FPCN nodes cluster into two separate families. (*B*) Surface rendering of FPCN nodes from the Yeo parcellation, color-coded based on the hierarchical clustering results. (*C*) Accuracy of the support vector machine classifier in distinguishing $FPCN_A$ and $FPCN_B$ FC patterns with the DN and DAN during each condition. Dotted line represents baseline accuracy (50%). (*D*) Surface rendering of FPCN nodes from the Gordon parcellation, color coded based on the hierarchical clustering results in *SI Appendix*, Fig. S3*B*. Abbreviations are the same as in Fig. 1.

chance level discrimination (~50% accuracy; *Materials and Methods*). A FPCN fractionation was also observed when using an independent set of nodes and network definitions based on the Gordon parcellation (57) (Fig. 1*D*) or Power parcellation (58) (*SI Appendix*, Fig. S1).

To further elucidate the origin of heterogeneity within the FPCN, we examined FPCN clustering patterns based strictly on FC with the DN and DAN. The results again revealed two distinct subsystems, identical to the structure observed based on intramodular connections (Fig. 2 and *SI Appendix*, Fig. S3). This suggests that the internal organization of the FPCN may be specifically related to connectional patterns with the DN and DAN. This provides a greater level of detail in understanding FPCN heterogeneity that goes beyond prior parcellations based on whole-brain FC patterns. The separation between $FPCN_A$ and $FPCN_B$ based on FC with the DN and DAN was highly consistent across participants, as evidenced by highly accurate discrimination when using a linear SVM classifier with fourfold cross-validation (Fig. 2*C* and *SI Appendix*, Fig. S4).

**Differential Coupling Patterns with the DN and DAN.** To visualize the basis of the FPCN fractionation, we used the Kamada–Kawai energy algorithm (59), which produces spring-embedded layouts that minimize the geometric distances of nodes based on their topological distances in the graph. Nodes are pulled together or pushed apart based on the strength of functional connections rather than anatomical locations. Visualization of the network topology revealed that $FPCN_A$ and $FPCN_B$ nodes were not intermingled, but rather, separated, with $FPCN_A$ nodes pulled toward DN nodes and $FPCN_B$ nodes pulled toward DAN nodes (Fig. 3).

The group-averaged correlation matrix revealed that $FPCN_A$ nodes exhibited positive correlations with DN nodes and no correlation or negative correlations with DAN nodes, whereas $FPCN_B$ nodes exhibited the opposite pattern (Fig. 4*A*; see also *SI Appendix*, Fig. S7). Furthermore, FC fingerprints (Fig. 4*B*) and whole-brain seed-based correlation maps (*SI Appendix*, Fig. S5) revealed that spatially adjacent $FPCN_A$ and $FPCN_B$ nodes exhibited divergent functional coupling patterns with DN and DAN regions. Thus, distinct FPCN subsystems can be delineated based on topographically organized functional connections with the DN and DAN.

*SI Appendix*, Fig. S6 illustrates the mean strength of FC between each pair of networks. In every condition we found a FPCN Subsystem × DN/DAN interaction [all $F(1, 22) > 70.49$, $P < 0.001$]. $FPCN_A$–DN coupling was stronger than $FPCN_B$–DN coupling [paired $t$ tests, all $t(23) > 8.62$, $P < 0.001$, Bonferroni corrected], whereas $FPCN_B$–DAN coupling was stronger than $FPCN_A$–DAN coupling [all $t(23) > 5.70$, $P < 0.001$, Bonferroni corrected]. To further quantify the strength of asymmetrical FC

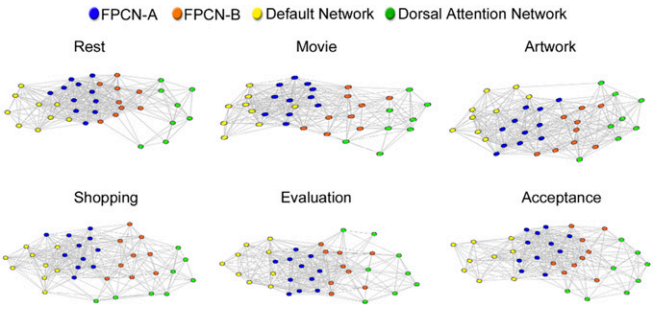


**Fig. 3.** Visualization of the network topology. FPCN nodes are color coded based on the hierarchical clustering analysis of intramodular connections. For each task, the group averaged FC matrix was thresholded to retain connections with $z(r) > 0.15$, and then submitted to the Kamada–Kawai energy algorithm, implemented in Pajek software. This algorithm produces spring-embedded layouts that minimize the geometric distances of nodes based on their topological distances in the graph. Well-connected nodes are pulled toward each other, whereas weakly connected nodes are pushed apart in a manner that minimizes the total energy of the system. In every context, there is a separation of FPCN nodes, with $FPCN_A$ nodes exhibiting preferential FC with DN nodes and $FPCN_B$ nodes exhibiting preferential FC with DAN nodes.

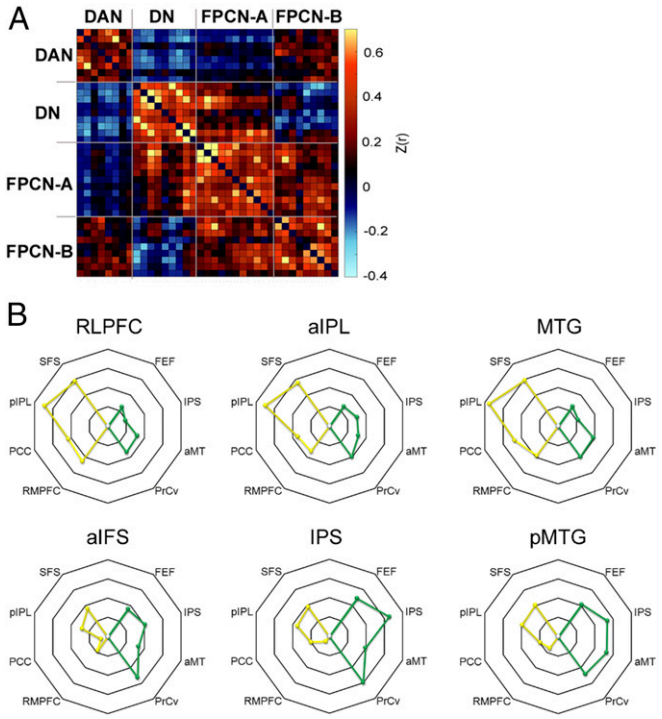


**Fig. 4.** Differential FPCN subsystem coupling patterns. (*A*) Group-averaged correlation matrix reflecting mean $z(r)$ values across the six task conditions, using Yeo parcellation nodes. (*B*) FC fingerprints for each FPCN node. In each case, the scale goes from $z(r) = -0.3$–$0.5$, in increments of 0.2. (*B*, *Top*) $FPCN_A$ nodes demonstrate a clear leftward bias, reflecting stronger FC with DN nodes (yellow data points). (*B*, *Bottom*) $FPCN_B$ nodes show a rightward bias, reflecting stronger FC with DAN nodes (green data points). $FPCN_A$ and $FPCN_B$ fingerprints are highly divergent for each pair of spatially adjacent nodes (*Top* vs. *Bottom* fingerprint). Abbreviations: aIFS, anterior inferior frontal sulcus; aIPL, anterior inferior parietal lobule; aMT, anterior middle temporal region.; FEFs, frontal eye fields; IPS, intraparietal sulcus; LTC, lateral temporal cortex; MFG, middle frontal gyrus; MTG, middle temporal gyrus; PCC, posterior cingulate cortex; pIFS, posterior inferior frontal sulcus; pIPL, posterior inferior parietal lobule; pMTG, posterior middle temporal gyrus; PrCv, ventral precentral cortex; RLPFC, rostrolateral prefrontal cortex; RMPFC, rostromedial prefrontal cortex; SFS, superior frontal suclus.

for each subsystem, we computed a "selectivity index" (SI), which reflected the relative degree of coupling with the DN versus DAN (*Materials and Methods*) (Fig. 5). The SI revealed that $FPCN_A$ nodes were more connected to the DN than DAN in every condition [all $t(23) > 4.07$, $P < 0.001$, Bonferroni corrected]. In contrast, $FPCN_B$ nodes were more connected to the DAN than DN in every condition [all $t(23) > 3.37$, $P < 0.02$, Bonferroni corrected]. Averaged across tasks, every individual FPCN node exhibited a significant SI [one-sample $t$ tests, all $t(23) > 3.23$, $P < 0.05$, false discovery rate (FDR) corrected], with the exception of the right posterior middle temporal gyrus (pMTG) ($P = 0.61$, FDR corrected) (*SI Appendix*, Fig. S7). Thus, asymmetrical FC with the DN versus DAN is widely present throughout the FPCN. The right middle frontal gyrus (MFG; area 9/46) exhibited the strongest SI, while the right pMTG exhibited the weakest SI, suggesting a more domain general profile. Averaged across tasks, asymmetrical FC was stronger for $FPCN_A$ than $FPCN_B$ [paired $t$ tests, $t(23) = 2.24$, $P = 0.057$], however, this effect was largely driven by the movie condition ($P = 0.003$, Bonferroni corrected; all other conditions, $P > 0.05$, Bonferroni corrected). While the DN core subsystem was our main focus, for completeness we also report the strength of asymmetry involving the other DN subsystems in *SI Appendix*, Fig. S8.

**Replication and Generalizability of Differential Coupling Patterns.** We next examined whether the fractionation would replicate in three independent datasets involving demanding cognitive control tasks that frequently activate the FPCN: rule use; Stroop; and 2-back working memory. We found a robust FPCN Subsystem × DN/DAN interaction in each task [rule use, $F(1, 13) = 75.10$, $P < 0.001$; Stroop, $F(1, 26) = 144.36$, $P < 0.001$; N-back, $F(1, 36) = 58.66$, $P < 0.001$]. In addition, we observed a significant selectivity index in each task, indicating that $FPCN_A$ was preferentially coupled with the DN (all $t > 3.61$, $P < 0.003$, Bonferroni corrected), and $FPCN_B$ was preferentially coupled with the DAN (all $t > 3.92$, $P < 0.002$, Bonferroni corrected) (Fig. 5*C*).

To examine the generalizability of the FPCN fractionation, we performed an automated meta-analysis on coactivation patterns across the wide range of tasks within the Neurosynth database (45). The results demonstrated that there are notable differences in coactivation with other parts of the brain between the two FPCN subsystems, consistent with our predictions (Fig. 6). In particular, $FPCN_A$ coactivates to a greater extent with the default network [e.g., rostromedial prefrontal cortex (PFC)], posterior cingulate cortex, and lateral temporal cortex), than does $FPCN_B$. There was less evidence for a distinction with respect to coactivation with the DAN. However, $FPCN_B$ does coactivate to a greater extent with portions of DAN around the superior parietal lobule and frontal eye fields.

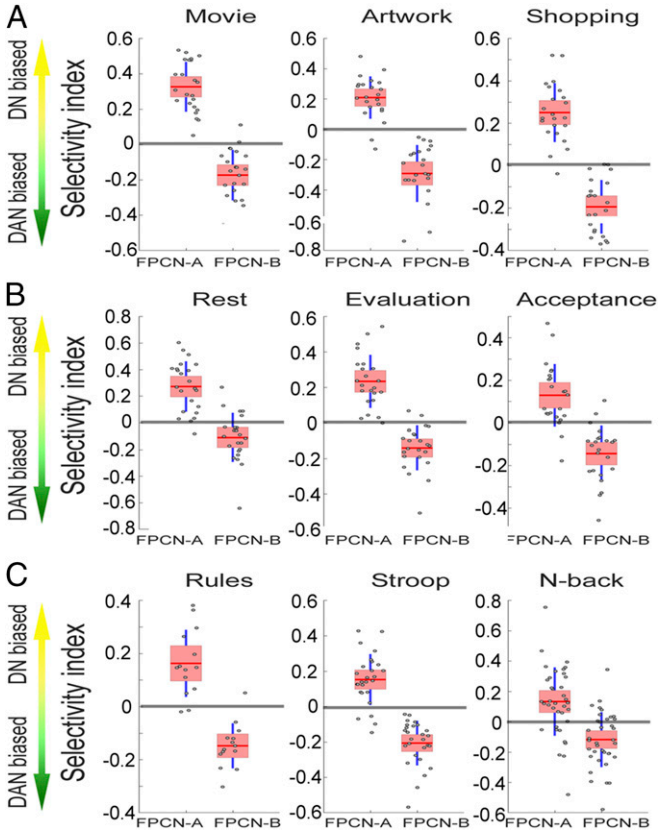


**Fig. 5.** Selectivity index (SI) for the FPCN subsystems during each condition, using Yeo parcellation nodes. The SI reflects mean functional connectivity (FC) with DN nodes minus mean FC with DAN nodes. (*A*) Tasks that involve external perceptual attention. (*B*) Tasks that involve internal attention. (*C*) Cognitive control tasks from the replication samples. Data for each participant (gray dots), with mean (white line), 95% CI (light-red shaded areas) and 1 SD (blue lines).

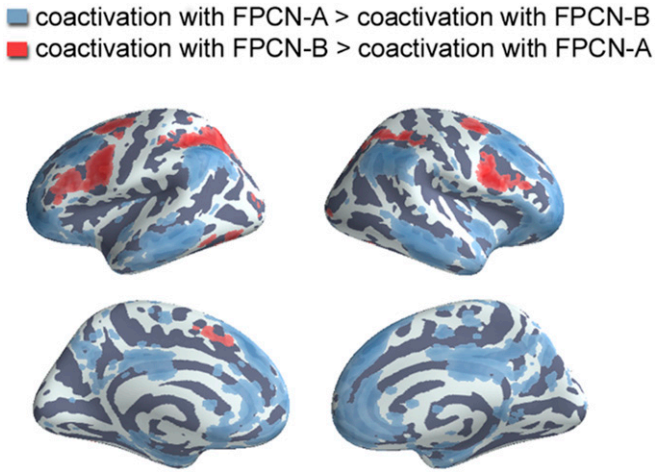


**Fig. 6.** Meta-analytic coactivation contrasts. Red voxels indicate significantly greater coactivation with $FPCN_B$ than $FPCN_A$. Blue voxels indicate significantly greater coactivation with $FPCN_A$ than $FPCN_B$. Images were whole-brain corrected using a false discovery rate of $q = 0.05$.

**Individual Network Mapping.** We next used hierarchical clustering to examine FPCN organization in each individual participant. This served to: (*i*) illustrate the extent of intersubject variability in the spatial organization of the FPCN subsystems and (*ii*) rule out the possibility that the group-level findings described thus far are biased by errors in spatial normalization. Voxels near the border of different networks in normalized space may potentially include a mixture of networks across different participants, and this may bias group-level results in the direction observed here, because $FPCN_A$ is adjacent to the DN, and $FPCN_B$ is adjacent to the DAN. This possibility can be ruled out if a fractionation is observed at the level of individual participants because there is complete segregation of all four networks. Importantly, the results demonstrated a fractionation of FPCN nodes into two clusters in every individual (Fig. 7 and *SI Appendix*, Fig. S9). While the spatial arrangement of $FPCN_A$ and $FPCN_B$ varies to some extent across individuals (as expected), there is a large degree of consistency across a number of regions. Moreover, in each case, $FPCN_A$ nodes are coupled with the DN but not DAN, whereas $FPCN_B$ nodes are coupled with the DAN but not DN (*SI Appendix*, Table S1). In most individuals, the rostrolateral prefrontal cortex, anterior inferior parietal lobule, presupplementary motor area, and middle temporal gyrus belong to $FPCN_A$, whereas the intraparietal sulcus, posterior inferior frontal sulcus/inferior frontal junction (IFS/IFJ), posterior superior frontal sulcus, and left posterior middle temporal gyrus belong to $FPCN_B$. Thus, differential connectivity with the DN and DAN is a property of FPCN organization and not driven by errors in spatial normalization.

**FPCN Heterogeneity and Task-Related Flexibility.** Prior work has shown that FPCN FC patterns exhibit a high-level of task-related flexibility (5, 7, 51). We examined how differential coupling patterns relate to FPCN flexibility. We computed a task-related "flexibility index" reflecting the extent to which FC patterns changed more across conditions than within conditions (i.e., from the first half to the second half of each condition). This measure of flexibility pertains to context and is different from the measure used by Bassett et al., which pertains to temporal flexibility (60). One-sample $t$ tests revealed that both subsystems exhibited a significant flexibility index, revealing task-dependent reconfiguration of FC patterns [$FPCN_A$, $t(22) = 8.26$, $P < 0.001$; $FPCN_B$, $t(22) = 9.35$, $P < 0.001$] (Fig. 8*A*). There was no difference between $FPCN_A$ and $FPCN_B$ in the strength of task-related flexibility (paired $t$ test, $P = 0.31$). Not only did overall FC patterns with the DN and DAN change across conditions for both subsystems, but so did the magnitude of the selectivity index—the relative strength of DN to DAN connections, evidenced by a main effect of task [$FPCN_A$, $F(5, 100) = 5.40$, $P < 0.001$; $FPCN_B$, $F(5, 100) = 6.00$, $P < 0.001$]. We found that the right IFS/IFJ node exhibited the greatest task-related flexibility (Fig. 8*B*). This region was positively coupled with the DAN in every condition, but more so in conditions that required external perceptual attention. Additionally, the IFS/IFJ flexibly shifted from negative coupling with DN nodes during task conditions involving external perceptual attention, to positive coupling with some DN nodes during task conditions that involved internal attention (Fig. 8 *C* and *D*). These observations were reflected in a significant task condition (internal vs. external) × network (DN vs. DAN) interaction, $F(8, 176) = 19.49$, $P < 0.001$. Thus, while $FPCN_A$ and $FPCN_B$ exhibited differential coupling patterns in every condition, the magnitude of this effect flexibly adapted to task demands.

**Are $FPCN_A$ and $FPCN_B$ Subsystems of the Same Network or Extensions of the DN and DAN?** To determine whether $FPCN_A$ and $FPCN_B$ should be considered subsystems within the same network or extensions of the DN and DAN, we compared mean between-network and between-subsystem FC patterns using paired $t$ tests. During the traditional cognitive control tasks, $FPCN_A$ and $FPCN_B$ exhibited stronger coupling with each other than with the DN [rule use, $t(13) = 3.11$, $P = 0.075$, Bonferroni corrected; Stroop, $t(26) = 6.50$, $P < 0.001$, Bonferroni corrected; 2-back, $t(36) = 3.26$, $P = 0.022$, Bonferroni corrected] or DAN [rule use, $t(13) = 5.76$, $P < 0.001$, Bonferroni corrected; Stroop, $t(26) = 6.82$, $P < 0.001$, Bonferroni corrected; 2-back, $t(36) = 4.20$, $P = 0.004$, Bonferroni corrected] (Fig. 9). However, the picture is less clear during the other conditions that involved a range of processing demands. Coupling between $FPCN_A$ and $FPCN_B$ was weaker than $FPCN_A$–DN coupling during the movie [$t(22) = 4.30$, $P < 0.05$, Bonferroni

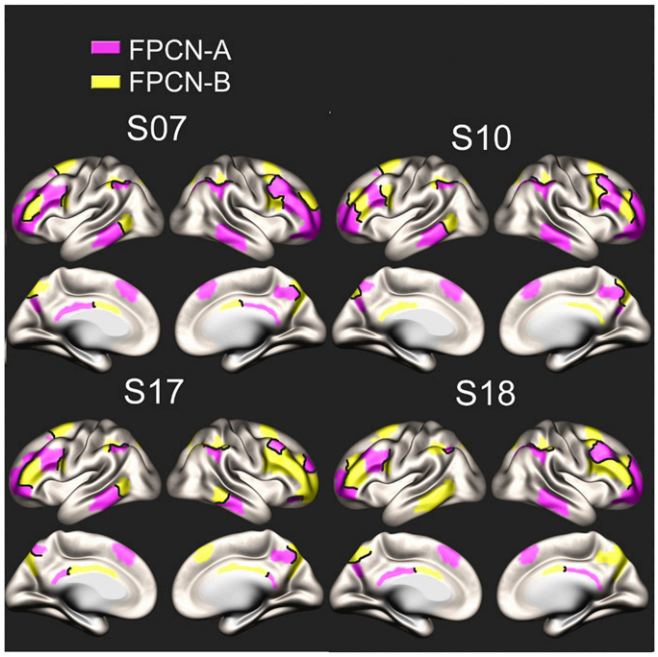


**Fig. 7.** FPCN organization in four individual participants. We color coded 66 FPCN nodes based on the results of a hierarchical clustering analysis. See *SI Appendix* for details about the nodes and analysis, and *SI Appendix*, Fig. S9 for maps of every participant.

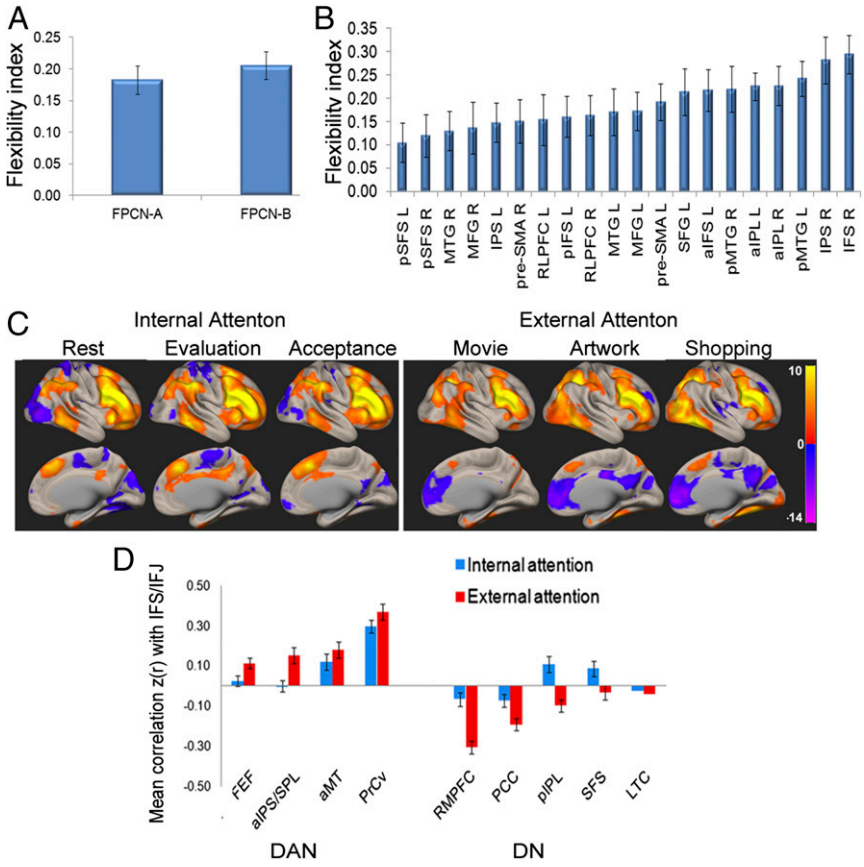


**Fig. 8.** Task-related flexibility of functional connectivity patterns. (*A*) Flexibility index reflecting the extent to which FC with the DN and DAN changes across contexts, using the Yeo parcellation nodes. Both $FPCN_A$ and $FPCN_B$ exhibit significant flexibility. (*B*) Flexibility index for each FPCN node. The right IFS/IFJ region of interest exhibited the greatest FC flexibility across conditions, consistent with prior work showing that the IFS/IFJ encodes task demands (3, 100) and contributes to the top-down control of attention (66) by shifting coupling patterns with different regions based on the target of attention (65). (*C*) IFS/IFJ seed maps for each condition. For illustration purposes, we use a slightly liberal threshold to show the full extent of positively and negatively correlated voxels ($Z > 2.57$, $P < 0.05$, FDR cluster corrected). (*D*) Mean FC between the IFS/IFJ and DN and DAN nodes. Error bars reflect between-subject SEM.

corrected] and shopping conditions [$t(23) = 3.27$, $P < 0.05$, Bonferroni corrected] but not different during the other conditions ($P > 0.05$, Bonferroni corrected). Coupling between $FPCN_A$ and $FPCN_B$ was stronger than $FPCN_B$–DAN coupling during rest [$t(23) = 9.82$, $P < 0.05$, Bonferroni corrected], evaluation [$t(23) = 5.15$, $P < 0.05$, Bonferroni corrected], and acceptance [$t(23) = 7.59$, $P < 0.05$, Bonferroni corrected], but not different during the other conditions ($P > 0.05$, Bonferroni corrected). These findings suggest that the extent to which the $FPCN_A$ and $FPCN_B$ cluster together versus with the DN/DAN depends on current processing demands.

**Meta-Analytic Functional Differentiation.** To examine whether the FPCN subsystem distinctions in network architecture are functionally meaningful, we used a naive Bayes classifier to determine which Neurosynth topics were preferentially associated with each subsystem. We plotted the loading of each topic onto each subsystem along with bootstrapped 95% confidence intervals (Fig. 10 and *SI Appendix*, Fig. S10). As expected, both subsystems showed high loadings to executive function topics, including working memory, switching, and conflict. Notably, there were also distinctions. The topics "mentalizing" and "emotion" loaded more strongly onto $FPCN_A$ than $FPCN_B$. In contrast, "attention," "action," "reading," and "semantics" loaded more strongly onto $FPCN_B$ than $FPCN_A$. These differences are consistent with the idea that $FPCN_A$ is biased toward functions that are associated with the DN, whereas $FPCN_B$ is biased toward functions that are associated with the DAN.

## Discussion

The current study provides evidence of highly reliable heterogeneity within the FPCN that is related to connectional patterns and functions associated with the DN and DAN—large-scale systems that contribute to introspective processes and visuospatial perceptual attention, respectively. To summarize: (*i*) hierarchical clustering revealed a separation of $FPCN_A$ and $FPCN_B$ nodes based on intramodular connections and intermodular connections with the DN and DAN; (*ii*) a linear SVM classifier was able to distinguish $FPCN_A$ and $FPCN_B$ FC patterns with remarkable accuracy; (*iii*) differential coupling patterns were replicated in three additional datasets; (*iv*) in every individual participant we observed a fractionation of the FPCN into two subsystems based on FC with the DN and DAN; (*v*) Neurosynth meta-analytic coactivation patterns revealed differential task-based coactivation with the DN and DAN; and (*vi*) there were differences in the task domains that predicted activation in $FPCN_A$ and $FPCN_B$. These findings offer a distinct perspective on the systems-level circuitry underlying executive control.

**Functional Organization of the FPCN.** Brain networks can be understood within the context of a hierarchical gradient of processing. At one extreme, unimodal sensorimotor regions process concrete sensory and action-related information, while at the

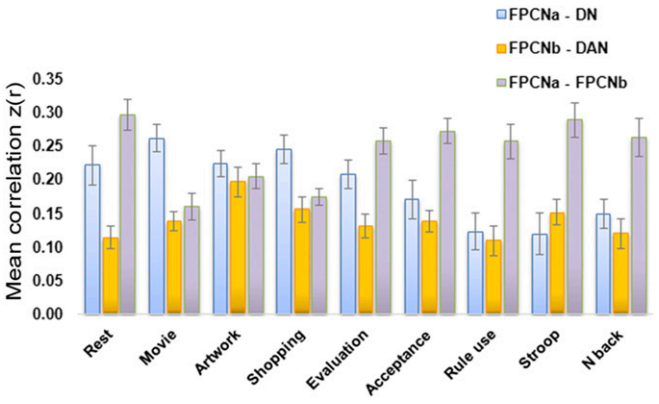


**Fig. 9.** Mean between-network FC in each condition.

other extreme, heteromodal regions elaborate upon such information, allowing for abstract thought, reasoning, and mental simulations of events (14–16). A number of important studies have shown that the primary functional distinction between the DAN and DN (22, 23, 61) is directly related to the brain's anatomical architecture, with DN regions being more physically remote from primary sensorimotor cortices (14). Our findings build upon this work and suggest that this distinction may be carried forward into the organization of the FPCN. This provides an understanding of how the FPCN and cognitive control may relate to perceptual versus introspective modes of processing.

The DAN is activated when attention is directed in a top-down manner to task-relevant objects and locations and also when intrinsically salient stimuli are detected (24–27, 29, 31, 62). Our findings suggest a close relationship between $FPCN_B$ and the DAN in the network topology. Moreover, we found that $FPCN_B$ was associated with functional domains that are known to activate the DAN. Specifically, $FPCN_B$ was significantly more associated with topics related to attention and action than $FPCN_A$. Prior work suggests that $FPCN_B$ contributes to cognitive control by flexibly encoding task-relevant information, including task rules (e.g., stimulus-response mappings) and their relationship to expected reward outcomes (2–4, 6, 63, 64). Notably, $FPCN_B$ regions including the inferior frontal junction play a causal top-down role in modulating the DAN and perceptual attention (65, 66). One possibility is that $FPCN_B$ represents information about task context in working memory and that the DAN translates this information into commands to guide the deployment of spatial attention to specific objects and locations (65, 66). By exerting top-down control over the DAN, $FPCN_B$ may ensure that attention remains focused on task-relevant perceptual information, rather than salient, yet irrelevant stimuli, or task-irrelevant thoughts. Thus, the role of $FPCN_B$ in executive control may be related to the abstraction, monitoring, and manipulation of sensorimotor contingencies to facilitate moment-to-moment interactions with the environment.

In contrast, $FPCN_A$ regions are activated when attention is directed toward one's own thoughts and away from perceptual inputs (67–69), for example, during tasks that require metacognitive awareness (67, 70, 71), relational reasoning (72, 73), multitasking and complex task sets (64, 74–77), stimulus-independent and abstract thinking (38, 68, 78–81), mentalizing (82), episodic memory (51, 83), future planning (5), and prospective memory (84). Consistent with this, we found that $FPCN_A$ was preferentially coupled with the DN, which plays a role in bringing conceptual–associative knowledge to bear on current thought and perception (33–35, 41, 85). Additionally, $FPCN_A$ was associated with functional domains that are known to activate the DN. Specifically, $FPCN_A$ was significantly more associated with topics related to mentalizing and emotion than $FPCN_B$. Thus, $FPCN_A$ may preferentially contribute to executive control in the context of introspective processes and enable modes of thought that are relatively free from the constraints of concrete sensorimotor interactions with the environment. A recent framework (41) suggests that $FPCN_A$ (in particular the rostrolateral prefrontal cortex), may contribute to the abstract "top-level management" of thought, exerting a general constraint that keeps one's focus on task-relevant material, yet allowing for some degree of spontaneous variability in thought. In this way, $FPCN_A$ may play a role in regulating internal thoughts and emotions in service of social reasoning, mental time travel (e.g., future goal planning), and metacognitive awareness of emotional states. It may also contribute to the performance of traditional cognitive control tasks by allowing representations of abstract task rules and temporally extended contexts to guide the implementation of more concrete rules and actions (76, 86–88).

In every condition, including demanding cognitive control tasks (rule use, Stroop, 2-back), we found robust coupling between $FPCN_A$ and the DN. Consistent with this, a recent study found encoding of task-relevant information by the DN and increased activation during demanding rule switches, suggesting that it may contribute to some forms of cognitive control that involve activating different cognitive contexts (89). We did find, however, that the magnitude of $FPCN_A$–DN coupling was reduced during the cognitive control tasks relative to other conditions,

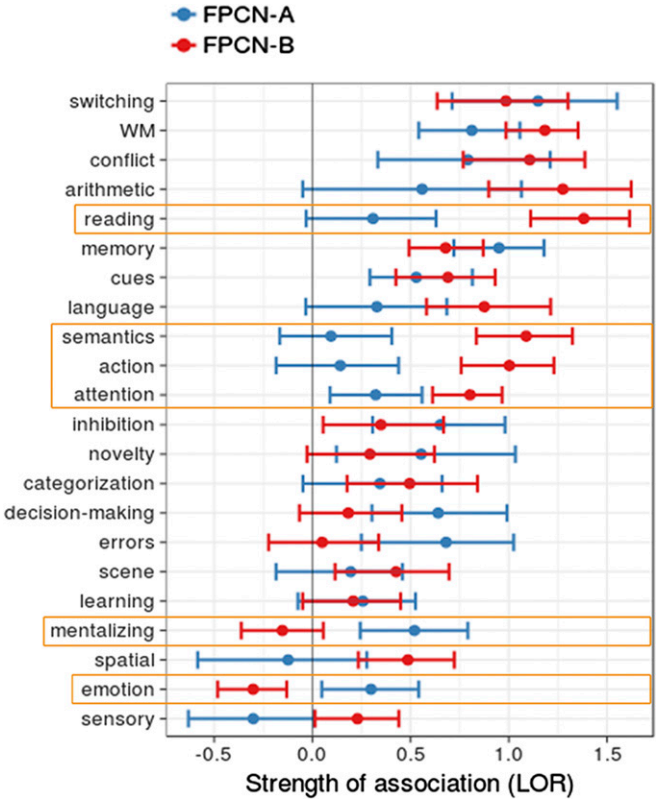


**Fig. 10.** Meta-analytic functional preference profile of FPCN subsystems. We trained naive Bayes classifiers to predict the presence or absence of activation in each FPCN subsystem using a set of 60 psychological topics and plotted topics that were significantly positively associated with at least one subsystem. Strength of association is measured in log odds ratio (LOR) with values greater than 0 indicating that the presence of that topic in a study positively predicts activity in a subsystem. Ninety-five percent confidence intervals derived using bootstrapping are indicated, and topics differentially associated with each system are highlighted in orange. WM, working memory.

and was significantly lower than $FPCN_A$–$FPCN_B$ coupling. $FPCN_A$ was strongly aligned with the DN across the six conditions in the primary dataset, which were designed to elicit mental states that resemble those frequently experienced in everyday life. Thus, the diminished relationship with the DN during the traditional cognitive control tasks may represent the exception rather than the rule. $FPCN_A$ may typically operate as an extension of the DN, but becomes coopted by $FPCN_B$ when it is necessary to perform highly complex perceptually focused tasks. Thus, while $FPCN_B$ may have evolved as an extension of the DAN processing stream to allow for the regulation of visuospatial perception and action during physical interactions with the environment (e.g., tool use), $FPCN_A$ may have evolved as an extension of the DN processing stream to allow for the regulation of introspective processes such as complex social reasoning. This proposal aligns with suggestion that there is an intimate relationship between brain evolution, including expansion of the anterior prefrontal cortex in humans (90), and the emergence of complex social life (91). Moreover, it has been suggested that some aspects of $FPCN_A$ anatomy may be unique to humans and may underlie our exceptional capacity for higher-order thought (73). However, the functional distinction between the FPCN subsystems suggested here is just a starting point; a more elaborate theoretical framework will be required as work on the FPCN progresses.

**Relation to Other Models of Executive Control and Frontoparietal Organization.** According to one model, the FPCN is critical for trial-by-trial adjustments in control, whereas a cingulo-opercular network is critical for the maintenance of task goals across trials, supporting a balance between flexibility and stability (1). Rapid adjustments in control may occur via flexible task-dependent shifts in FPCN coupling patterns (5, 7, 51). Another model suggests that the salience network initiates shifts in modes of information processing related to the FPCN and DN (92). Our findings suggest an orthogonal dimension of executive control, with different zones within the FPCN involved in visuospatial attention and introspective processes. Broadly consistent with this idea, a prior study revealed a functional distinction between these subsystems that is relevant for understanding their contributions to cognitive control. In particular, $FPCN_A$ regions were associated with resolving uncertainty when monitoring internally maintained task sequences, whereas $FPCN_B$ regions were more associated with task complexity and execution (i.e., the number of rule switches vs. rule repeats) (93). Recent work suggests a distance from sensory-motor processing organizational principle, with more complex and abstract processing occurring in regions that are physically remote from primary sensory and motor cortices (14, 16). Our findings suggest that $FPCN_A$ may be further removed from sensory-motor processing than $FPCN_B$. Consistent with this, we observed that $FPCN_A$ but not $FPCN_B$ nodes were negatively correlated with primary sensory-motor regions (*SI Appendix*, Fig. S5). Thus, a general principle of functional organization may apply across different brain networks (14) and within the FPCN itself.

Other work has emphasized that the FPCN is a flexible hub that coordinates processing across other networks in a task-dependent manner (5, 7, 94). In the current study, we found that $FPCN_A$ and $FPCN_B$ were generally aligned with the DN and DAN, respectively; however, there was also evidence that FC patterns flexibly adapted to task demands. There were overall shifts in $FPCN_A$ and $FPCN_B$ coupling patterns, as well as shifts in the relative "preference" of coupling with the DN versus DAN. The right IFS/IFJ node of $FPCN_B$ exhibited the strongest task-related flexibility and was positively coupled with both DAN and DN regions in some contexts. These findings are compatible with evidence of adaptive coding properties in FPCN neurons (2) and suggest that some FPCN nodes may be relatively domain general in nature, consistent with the notion of a multiple demand system (4). The organization noted here is thus fully compatible with findings of task-dependent reconfiguration of FPCN FC patterns. Additionally, some conceptions of the multiple demand network emphasize $FPCN_B$ regions. The finding that some $FPCN_B$ nodes are especially flexible is consistent with this work. To summarize, we suggest that asymmetrical coupling patterns reflect a relative and flexible difference between $FPCN_A$ and $FPCN_B$, rather than an absolute and fixed aspect of network architecture.

**Limitations.** One of the challenges in examining heterogeneity within the FPCN it how to define this network to begin with. Rather than select a single method, we used nodes based on three different parcellations (Yeo, Gordon, and Power) that identified the FPCN as a functional unit on the level of other functional systems (e.g., visual and somatomotor networks). We then looked for finer-grained heterogeneity within this system. While there was broad agreement across parcellations in terms of the location of nodes exhibiting preferential coupling with the DN versus DAN, there were also some differences. To some extent, these differences arise from how the FPCN (as a whole network) was defined in each case. Additionally, we observed individual variation in the precise location of regions showing a bias toward the DN or DAN. Indeed, the broad domain generality of the FPCN (95) may lead to slight differences across individuals in the spatial distribution of axonal projections to and from the DN and DAN during development. Thus, while our findings suggest FPCN nodes show a relative bias in connectivity toward the DN or DAN, it is important to note that we are not arguing for a precise anatomical demarcation of two FPCN subsystems. A second issue is that our range of tasks was not exhaustive, making it possible that different network interactions could be observed in some contexts (e.g., positive coupling between the $FPCN_A$ and DAN). One instance may be perceptual metacognition, which is known to rely on parts of the $FPCN_A$, including the rostrolateral prefrontal cortex (70). Additionally, it is possible that the FPCN may not fractionate, but rather, serve as a domain general resource during demanding tasks that require considerable effort (4). However, our findings do suggest that a FPCN fractionation can be observed in many diverse contexts. Finally, our analysis is limited by the reliance on predefined network boundaries and the assumption of discrete brain clusters/networks. Any brain parcellation is a dimensionality reduction on a complex space and should be viewed as a general guiding principle rather than a set of fixed and precise brain network demarcations. Moreover, the network affiliation of a given brain region can shift across time and context (60, 96). That being said, our results provide evidence that spatially distinct parts of the FPCN—as defined using three different parcellations—are differentially coupled with the DN and DAN across a range of contexts.

## Conclusions

Executive control processes are multifaceted and likely rely on multiple interacting, yet distinct neural systems. The current work makes a step forward in discerning the network basis of executive control and may offer predictions about clinical deficits in control functions. For example, altered connectivity between $FPCN_A$ and the DN may interfere with regulating self-referential thoughts in conditions such as depression, whereas altered connectivity between $FPCN_B$ and the DAN may interfere with regulating visuospatial attention (e.g., focusing on goal-relevant objects) in conditions such as ADHD.

## Materials and Methods

See *SI Appendix* for complete details regarding data preprocessing and analysis. Participants in the primary dataset (sample 1) were 24 healthy adults (mean age = 30.33, SD = 4.80; 10 female; 22 right-handed), with no history of head trauma or psychological conditions. This study was approved

by the University of British Columbia Clinical Research Ethics Board, and all participants provided written informed consent, and received payment ($20/h) for their participation. Due to a technical error, data for the movie and acceptance-based introspection conditions were not collected for one participant. At the end of scanning, one participant reported experiencing physical discomfort throughout the scan. Similar results were obtained with or without inclusion of this participant's data, so they were included in the final analysis. Data for one participant was not included due to excessive motion. This resulted in a final sample size of 23.

**Primary Dataset Task Conditions.** The primary dataset included six ecologically valid task conditions in separate 6-min fMRI runs. Each task condition was designed to elicit a continuous mental state and did not require any responses. (*i*) Resting state. Participants lay in the scanner with their eyes closed and were instructed to relax and stay awake and to allow their thoughts to flow naturally. (*ii*) Movie watching. Participants watched a clip from the movie *Star Wars: Return of the Jedi* and were instructed to pay attention to the actions of the characters, and also to what they may be thinking and feeling. (*iii*) Artwork analysis. Participants viewed four pieces of artwork in the scanner, each for 90 s. These pieces were preselected by participants, and during scanning, they were instructed to pay attention to the perceptual details of the art, their inner experience (i.e., thoughts and feelings). (*iv*) Shopping task. While in the scanner, participants viewed a prerecorded video shot from a first-person perspective of items within several stores in a shopping mall. They were told to imagine that they are going through the mall to find a birthday gift for a friend and to analyze each item in terms of suitability based on their friend's preferences. (*v*) Evaluation-based introspection. Participants were asked to think about a mildly upsetting issue involving a specific person in their life (e.g., a friend, roommate, sibling, or partner), and asked to reflect on what the person and situation means to them, what has happened in the past and may happen in the future, and to analyze everything that is good or bad about the situation. (*vi*) Acceptance-based introspection. Participants were asked to reflect on the same upsetting issue as in the previous case, but this time were instructed to focus on moment-to-moment viscerosomatic sensation, and to accept these sensations without any judgment or elaborative mental analysis.

**Replication Datasets.** We examined the generalizability of our results in several additional (nonoverlapping) samples. Sample 2 ($n = 15$) performed a rule-based cognitive control task that has been described in full elsewhere (3). Briefly, participants used one of two rules (male/female face discrimination or abstract/concrete word meaning discrimination) to respond to visual stimuli on each trial. On some trials subjects could earn money by responding quickly and accurately. The rules switched from trial to trial requiring participants to actively represent and flexibly switch between the different rules. Data from a single run (run 1 of 6) were analyzed; we did this to be consistent with the other conditions, which involved data collected from a single run. Sample 3 ($n = 28$) performed a color-word version of the Stroop task with three conditions (congruent, incongruent, and neutral) and were instructed to ignore the meaning of the printed word and respond to the ink color in which the word was printed. Data were acquired in a single run and accessed from the OpenfMRI database (accession no. ds000164) (97). Sample 4 ($n = 41$) performed an N-back working memory task. Data were accessed from the OpenfMRI database (accession no. ds000115) (98). We analyzed the data from the task period during the demanding 2-back block in control participants, during which they determined whether each letter was the same as the letter shown two trials previously.

**Hierarchical Clustering Analysis.** We first created a group-averaged correlation matrix reflecting mean FC across all participants and all six conditions in the primary dataset. We then extracted the subgraph composed of within-FPCN FC values and the subgraph composed of FPCN connections with the DN and DAN. These subgraphs were separately submitted to the hierarchical clustering algorithm (cluster v3.0, 1988, Stanford University), which used Spearman correlation to determine distance and the average linkage method to cluster nodes.

**SVM Classification Analysis.** The SVM classifier was implemented with RapidMiner software (99). The cost parameter, C, was set to 1, and the convergence epsilon was set to 0.001. For each participant, we created a vector consisting of $FPCN_A$ correlations (with other FPCN nodes or with DN and DAN nodes), and a vector consisting of $FPCN_B$ correlations. The correlation vectors served as input features and were assigned a value of 1 or −1 to specify the FPCN subsystem to which they belonged. We tested the accuracy of the classifier using fourfold cross-validation. We did not perform any type of iterative optimization or feature selection, which should minimize the chance of overfitting. Permutation testing was used to obtain baseline classification accuracy.

**Quantifying the Strength of Asymmetrical FC Patterns.** To quantify the strength of asymmetrical DN and DAN connections for $FPCN_A$ and $FPCN_B$, we computed a selectivity index. For each participant, we first computed the averaged strength of FC between each FPCN node and the DN and the average strength of FC between each FPCN node and the DAN. This was done by computing the mean of all relevant Fisher *r*-to-*z* transformed correlation values. We then subtracted mean FC with the DAN from mean FC with the DN. This difference score served as the selectivity index. We averaged across values for all $FPCN_A$ nodes and all $FPCN_B$ nodes to derive the mean selectivity index for each subsystem.

**Analysis.** Data and code to perform analyses is available at: https://github.com/matthewldixon/FPCN_Heterogeneity. Additionally, Jupyter notebooks with analysis code and data for the Neurosynth analyses are available at: https://github.com/adelavega/fpcn_fractionation.


1. Dosenbach NU, et al. (2006) A core system for the implementation of task sets. *Neuron* 50:799–812.
2. Stokes MG, et al. (2013) Dynamic coding for cognitive control in prefrontal cortex. *Neuron* 78:364–375.
3. Dixon ML, Christoff K (2012) The decision to engage cognitive control is driven by expected reward-value: Neural and behavioral evidence. *PLoS One* 7:e51637.
4. Duncan J (2010) The multiple-demand (MD) system of the primate brain: Mental programs for intelligent behaviour. *Trends Cogn Sci* 14:172–179.
5. Spreng RN, Stevens WD, Chamberlain JP, Gilmore AW, Schacter DL (2010) Default network activity, coupled with the frontoparietal control network, supports goal-directed cognition. *Neuroimage* 53:303–317.
6. Miller EK, Cohen JD (2001) An integrative theory of prefrontal cortex function. *Annu Rev Neurosci* 24:167–202.
7. Cole MW, et al. (2013) Multi-task connectivity reveals flexible hubs for adaptive task control. *Nat Neurosci* 16:1348–1355.
8. Cole MW, Repovš G, Anticevic A (2014) The frontoparietal control system: A central role in mental health. *Neuroscientist* 20:652–664.
9. Andrews-Hanna JR, Reidler JS, Sepulcre J, Poulin R, Buckner RL (2010) Functional-anatomic fractionation of the brain's default network. *Neuron* 65:550–562.
10. Seeley WW, et al. (2007) Dissociable intrinsic connectivity networks for salience processing and executive control. *J Neurosci* 27:2349–2356.
11. Dosenbach NU, et al. (2007) Distinct brain networks for adaptive and stable task control in humans. *Proc Natl Acad Sci USA* 104:11073–11078.
12. Yeo BT, et al. (2011) The organization of the human cerebral cortex estimated by intrinsic functional connectivity. *J Neurophysiol* 106:1125–1165.
13. Braga RM, Buckner RL (2017) Parallel interdigitated distributed networks within the individual estimated by intrinsic functional connectivity. *Neuron* 95:457–471.e5.
14. Margulies DS, et al. (2016) Situating the default-mode network along a principal gradient of macroscale cortical organization. *Proc Natl Acad Sci USA* 113:12574–12579.
15. Mesulam MM (1998) From sensation to cognition. *Brain* 121:1013–1052.
16. Taylor P, Hobbs JN, Burroni J, Siegelmann HT (2015) The global landscape of cognition: Hierarchical aggregation as an organizational principle of human cortical networks and functions. *Sci Rep* 5:18112.
17. Fuster JM (2001) The prefrontal cortex–An update: Time is of the essence. *Neuron* 30:319–333.
18. Spreng RN, Sepulcre J, Turner GR, Stevens WD, Schacter DL (2013) Intrinsic architecture underlying the relations among the default, dorsal attention, and frontoparietal control networks of the human brain. *J Cogn Neurosci* 25:74–86.
19. Fox MD, et al. (2005) The human brain is intrinsically organized into dynamic, anticorrelated functional networks. *Proc Natl Acad Sci USA* 102:9673–9678.
20. Dixon ML, et al. (2017) Interactions between the default network and dorsal attention network vary across default subsystems, time, and cognitive states. *Neuroimage* 147:632–649.
21. Raichle ME (2015) The brain's default mode network. *Annu Rev Neurosci* 38:433–447.
22. Sestieri C, Shulman GL, Corbetta M (2010) Attention to memory and the environment: Functional specialization and dynamic competition in human posterior parietal cortex. *J Neurosci* 30:8445–8456.
23. Kelly AM, Uddin LQ, Biswal BB, Castellanos FX, Milham MP (2008) Competition between functional brain networks mediates behavioral variability. *Neuroimage* 39:527–537.
24. Corbetta M, Shulman GL (2002) Control of goal-directed and stimulus-driven attention in the brain. *Nat Rev Neurosci* 3:201–215.
25. Buschman TJ, Kastner S (2015) From behavior to neural dynamics: An integrated theory of attention. *Neuron* 88:127–144.
26. Ptak R (2012) The frontoparietal attention network of the human brain: Action, saliency, and a priority map of the environment. *Neuroscientist* 18:502–515.
27. Moore T, Armstrong KM (2003) Selective gating of visual signals by microstimulation of frontal cortex. *Nature* 421:370–373.
28. Corbetta M, et al. (1998) A common network of functional areas for attention and eye movements. *Neuron* 21:761–773.

29. Bisley JW, Goldberg ME (2003) Neuronal activity in the lateral intraparietal area and spatial attention. *Science* 299:81–86.
30. Buschman TJ, Miller EK (2007) Top-down versus bottom-up control of attention in the prefrontal and posterior parietal cortices. *Science* 315:1860–1862.
31. Gottlieb JP, Kusunoki M, Goldberg ME (1998) The representation of visual salience in monkey parietal cortex. *Nature* 391:481–484.
32. Ptak R, Schnider A, Fellrath J (2017) The dorsal frontoparietal network: A core system for emulated action. *Trends Cogn Sci* 21:589–599.
33. Buckner RL, Andrews-Hanna JR, Schacter DL (2008) The brain's default network: Anatomy, function, and relevance to disease. *Ann N Y Acad Sci* 1124:1–38.
34. Andrews-Hanna JR, Smallwood J, Spreng RN (2014) The default network and self-generated thought: Component processes, dynamic control, and clinical relevance. *Ann N Y Acad Sci* 1316:29–52.
35. Konishi M, McLaren DG, Engen H, Smallwood J (2015) Shaped by the past: The default mode network supports cognition that is independent of immediate perceptual input. *PLoS One* 10:e0132209.
36. Spreng RN, Mar RA, Kim AS (2009) The common neural basis of autobiographical memory, prospection, navigation, theory of mind, and the default mode: A quantitative meta-analysis. *J Cogn Neurosci* 21:489–510.
37. Andrews-Hanna JR, Saxe R, Yarkoni T (2014) Contributions of episodic retrieval and mentalizing to autobiographical thought: Evidence from functional neuroimaging, resting-state connectivity, and fMRI meta-analyses. *Neuroimage* 91:324–335.
38. Fox K, Spreng RN, Ellamil M, Andrews-Hanna JR, Christoff K (2015) The wandering brain: Meta-analysis of functional neuroimaging studies of mind-wandering and related spontaneous thought processes. *Neuroimage* 111:611–621.
39. Christoff K, Gordon AM, Smallwood J, Smith R, Schooler JW (2009) Experience sampling during fMRI reveals default network and executive system contributions to mind wandering. *Proc Natl Acad Sci USA* 106:8719–8724.
40. Ellamil M, et al. (2016) Dynamics of neural recruitment surrounding the spontaneous arising of thoughts in experienced mindfulness practitioners. *Neuroimage* 136: 186–196.
41. Christoff K, Irving ZC, Fox KC, Spreng RN, Andrews-Hanna JR (2016) Mind-wandering as spontaneous thought: A dynamic framework. *Nat Rev Neurosci* 17:718–731.
42. Denny BT, Kober H, Wager TD, Ochsner KN (2012) A meta-analysis of functional neuroimaging studies of self- and other judgments reveals a spatial gradient for mentalizing in medial prefrontal cortex. *J Cogn Neurosci* 24:1742–1752.
43. Barrett LF, Satpute AB (2013) Large-scale brain networks in affective and social neuroscience: Towards an integrative functional architecture of the brain. *Curr Opin Neurobiol* 23:361–372.
44. Dixon ML, Thiruchselvam R, Todd R, Christoff K (2017) Emotion and the prefrontal cortex: An integrative review. *Psychol Bull* 143:1033–1081.
45. Yarkoni T, Poldrack RA, Nichols TE, Van Essen DC, Wager TD (2011) Large-scale automated synthesis of human functional neuroimaging data. *Nat Methods* 8:665–670.
46. Hutchison RM, et al. (2013) Dynamic functional connectivity: Promise, issues, and interpretations. *Neuroimage* 80:360–378.
47. Bassett DS, Wymbs NF, Porter MA, Mucha PJ, Grafton ST (2014) Cross-linked structure of network evolution. *Chaos* 24:013112.
48. Zalesky A, Fornito A, Cocchi L, Gollo LL, Breakspear M (2014) Time-resolved resting-state brain networks. *Proc Natl Acad Sci USA* 111:10341–10346.
49. Betzel RF, Fukushima M, He Y, Zuo XN, Sporns O (2016) Dynamic fluctuations coincide with periods of high and low modularity in resting-state functional brain networks. *Neuroimage* 127:287–297.
50. Gonzalez-Castillo J, Bandettini PA (2017) Task-based dynamic functional connectivity: Recent findings and open questions. *Neuroimage*, 10.1016/j.neuroimage.2017.08.006.
51. Fornito A, Harrison BJ, Zalesky A, Simons JS (2012) Competitive and cooperative dynamics of large-scale brain functional networks supporting recollection. *Proc Natl Acad Sci USA* 109:12788–12793.
52. Braun U, et al. (2015) Dynamic reconfiguration of frontal brain networks during executive cognition in humans. *Proc Natl Acad Sci USA* 112:11678–11683.
53. Whitfield-Gabrieli S, Nieto-Castanon A (2012) Conn: A functional connectivity toolbox for correlated and anticorrelated brain networks. *Brain Connect* 2:125–141.
54. Murphy K, Birn RM, Handwerker DA, Jones TB, Bandettini PA (2009) The impact of global signal regression on resting state correlations: Are anti-correlated networks introduced? *Neuroimage* 44:893–905.
55. Fornito A, Zalesky A, Bullmore E (2016) *Fundamentals of Brain Network Analysis* (Academic, New York).
56. Rubinov M, Sporns O (2010) Complex network measures of brain connectivity: Uses and interpretations. *Neuroimage* 52:1059–1069.
57. Gordon EM, et al. (2016) Generation and evaluation of a cortical area parcellation from resting-state correlations. *Cereb Cortex* 26:288–303.
58. Power JD, et al. (2011) Functional network organization of the human brain. *Neuron* 72:665–678.
59. Kamada T, Kawai S (1989) An algorithm for drawing general undirected graphs. *Inf Process Lett* 31:7–15.
60. Bassett DS, et al. (2011) Dynamic reconfiguration of human brain networks during learning. *Proc Natl Acad Sci USA* 108:7641–7646.
61. Golland Y, et al. (2007) Extrinsic and intrinsic systems in the posterior cortex of the human brain revealed during natural sensory stimulation. *Cereb Cortex* 17:766–777.
62. Kastner S, Pinsk MA, De Weerd P, Desimone R, Ungerleider LG (1999) Increased activity in human visual cortex during directed attention in the absence of visual stimulation. *Neuron* 22:751–761.
63. Bunge SA, Kahn I, Wallis JD, Miller EK, Wagner AD (2003) Neural circuits subserving the retrieval and maintenance of abstract rules. *J Neurophysiol* 90:3419–3428.
64. Cole MW, Bagic A, Kass R, Schneider W (2010) Prefrontal dynamics underlying rapid instructed task learning reverse with practice. *J Neurosci* 30:14245–14254.
65. Baldauf D, Desimone R (2014) Neural mechanisms of object-based attention. *Science* 344:424–427.
66. Bichot NP, Heard MT, DeGennaro EM, Desimone R (2015) A source for feature-based attention in the prefrontal cortex. *Neuron* 88:832–844.
67. McCaig RG, Dixon M, Keramatian K, Liu I, Christoff K (2011) Improved modulation of rostrolateral prefrontal cortex using real-time fMRI training and meta-cognitive awareness. *Neuroimage* 55:1298–1305.
68. Burgess PW, Dumontheil I, Gilbert SJ (2007) The gateway hypothesis of rostral prefrontal cortex (area 10) function. *Trends Cogn Sci* 11:290–298.
69. Christoff K, Gabrieli JDE (2000) The frontopolar cortex and human cognition: Evidence for a rostrocaudal hierarchical organization within the human prefrontal cortex. *Psychobiology (Austin Tex)* 28:168–186.
70. Fleming SM, Weil RS, Nagy Z, Dolan RJ, Rees G (2010) Relating introspective accuracy to individual differences in brain structure. *Science* 329:1541–1543.
71. Baird B, Smallwood J, Gorgolewski KJ, Margulies DS (2013) Medial and lateral networks in anterior prefrontal cortex support metacognitive ability for memory and perception. *J Neurosci* 33:16657–16665.
72. Christoff K, et al. (2001) Rostrolateral prefrontal cortex involvement in relational integration during reasoning. *Neuroimage* 14:1136–1149.
73. Vendetti MS, Bunge SA (2014) Evolutionary and developmental changes in the lateral frontoparietal network: A little goes a long way for higher-level cognition. *Neuron* 84:906–917.
74. Koechlin E, Basso G, Pietrini P, Panzer S, Grafman J (1999) The role of the anterior prefrontal cortex in human cognition. *Nature* 399:148–151.
75. Braver TS, Bongiolatti SR (2002) The role of frontopolar cortex in subgoal processing during working memory. *Neuroimage* 15:523–536.
76. Nee DE, D'Esposito M (2016) The hierarchical organization of the lateral prefrontal cortex. *Elife* 5:e12112.
77. Sakai K (2008) Task set and prefrontal cortex. *Annu Rev Neurosci* 31:219–245.
78. Christoff K, Ream JM, Geddes LP, Gabrieli JD (2003) Evaluating self-generated information: Anterior prefrontal contributions to human cognition. *Behav Neurosci* 117:1161–1168.
79. Dixon ML, et al. (2017) Heterogeneity within the frontoparietal control network and its relationship to the default and dorsal attention networks. *bioRxiv*, 10.1101/178863.
80. Smallwood J, Brown K, Baird B, Schooler JW (2012) Cooperation between the default mode network and the frontal-parietal network in the production of an internal train of thought. *Brain Res* 1428:60–70.
81. Christoff K, Keramatian K, Gordon AM, Smith R, Mädler B (2009) Prefrontal organization of cognitive control according to levels of abstraction. *Brain Res* 1286: 94–105.
82. Bhatt MA, Lohrenz T, Camerer CF, Montague PR (2010) Neural signatures of strategic types in a two-person bargaining game. *Proc Natl Acad Sci USA* 107: 19720–19725.
83. Gilbert SJ, et al. (2006) Functional specialization within rostral prefrontal cortex (area 10): A meta-analysis. *J Cogn Neurosci* 18:932–948.
84. Poppenk J, Moscovitch M, McIntosh AR, Ozcelik E, Craik FI (2010) Encoding the future: Successful processing of intentions engages predictive brain networks. *Neuroimage* 49:905–913.
85. Spreng RN, et al. (2014) Goal-congruent default network activity facilitates cognitive control. *J Neurosci* 34:14108–14114.
86. Cole MW, Laurent P, Stocco A (2013) Rapid instructed task learning: A new window into the human brain's unique capacity for flexible cognitive control. *Cogn Affect Behav Neurosci* 13:1–22.
87. Badre D, D'Esposito M (2009) Is the rostro-caudal axis of the frontal lobe hierarchical? *Nat Rev Neurosci* 10:659–669.
88. Koechlin E, Summerfield C (2007) An information theoretical approach to prefrontal executive function. *Trends Cogn Sci* 11:229–235.
89. Crittenden BM, Mitchell DJ, Duncan J (2015) Recruitment of the default mode network during a demanding act of executive control. *Elife* 4:e06481.
90. Teffer K, Semendeferi K (2012) Human prefrontal cortex: Evolution, development, and pathology. *Prog Brain Res* 195:191–218.
91. Dunbar RI, Shultz S (2007) Evolution in the social brain. *Science* 317:1344–1347.
92. Sridharan D, Levitin DJ, Menon V (2008) A critical role for the right fronto-insular cortex in switching between central-executive and default-mode networks. *Proc Natl Acad Sci USA* 105:12569–12574.
93. Desrochers TM, Chatham CH, Badre D (2015) The necessity of rostrolateral prefrontal cortex for higher-level sequential behavior. *Neuron* 87:1357–1368.
94. Cocchi L, Zalesky A, Fornito A, Mattingley JB (2013) Dynamic cooperation and competition between brain systems during cognitive control. *Trends Cogn Sci* 17: 493–501.
95. de la Vega A, Yarkoni T, Wager TD, Banich MT (2017) Large-scale meta-analysis suggests low regional modularity in lateral frontal cortex. *Cereb Cortex*, 10.1093/cercor/bhx204.
96. Pessoa L (2015) Precis of the cognitive-emotional brain. *Behav Brain Sci* 38:e71.
97. Verstynen TD (2014) The organization and dynamics of corticostriatal pathways link the medial orbitofrontal cortex to future behavioral responses. *J Neurophysiol* 112: 2457–2469.
98. Repovš G, Barch DM (2012) Working memory related brain network connectivity in individuals with schizophrenia and their siblings. *Front Hum Neurosci* 6:137.
99. Hofmann M, Klinkenberg R (2013) *RapidMiner: Data Mining Use Cases and Business Analytics Applications* (CRC Press, Boca Raton, FL).
100. Brass M, Derrfuss J, Forstmann B, von Cramon DY (2005) The role of the inferior frontal junction area in cognitive control. *Trends Cogn Sci* 9:314–316.